Semiconductor Physics, Quantum Electronics & Optoelectronics, 2024. V. 27, No 4. P. 404-411.

Semiconductor physics

X-ray diffraction and Raman spectroscopy studies of Ga-Ge-Te alloys

A.V. Stronski[1], K.V. Shportko[1], H.K. Kochubei[1], M.V. Popovych[1], A.A. Lotnyk[2]

[1]V. Lashkaryov Institute of Semiconductor Physics, NAS of Ukraine, 41 Nauky Avenue, 03028 Kyiv, Ukraine
[2]Leibniz Institute of Surface Engineering, 15 Permoser Street, 04318 Leipzig, Germany
Corresponding author e-mail: k.shportko@ukr.net

Abstract. The structure and vibrational properties of glassy $Ge_{19}Te_{81}$ and $Ga_{7.9}Ge_{11.5}Te_{80.6}$ alloys were studied using X-ray diffraction and Raman spectroscopy. The amorphous nature of the obtained alloys was confirmed by the experimental X-ray diffraction patterns. The latter were used for calculating radial distribution functions. Such calculations gave the positions of the nearest-neighbour peak r_1 – 2.65 Å and second nearest-neighbour peak r_2 – 4.31 and 4.44 Å. The obtained r_1 values are in good agreement with the known from literature Ge-Te and Ga-Te bond lengths. Similar r_1 values were also observed for Ga-Ge-Te glasses of different compositions. The r_2/r_1 values of 1.63 and 1.68 are close to the typical value for a regular tetrahedron structure. The observed bands in the Raman spectra of the studied Ga-Ge-Te samples show that such glasses contain different nanophases. The Raman spectra may be interpreted in terms of vibrational modes of Ga-Te and Ge-Te binary glasses and films.

Keywords: X-ray diffraction, Raman spectroscopy, glassy Ga-Ge-Te alloys.

https://doi.org/10.15407/spqeo27.04.404
PACS 42.70.Ce, 61.43.Dq, 78.30.Er

Manuscript received 27.08.24; revised version received 01.10.24; accepted for publication 13.11.24; published online 06.12.24.

1. Introduction

Chalcogenide glasses are highly valued for their diverse scientific and technological applications, including memory switching, optical storage, holography, thermal imaging, night vision, biosensing, space exploration, medical diagnostics, and environmental monitoring [1–6]. Among the unique characteristics of chalcogenide glasses, a wide range of optical transparency, high values of linear and non-linear refractive index, photo-structural transformations accompanied by changes of optical and chemical properties [2], photo-induced effects such as photo-darkening and bleaching, local expansion or contraction, changes of the refractive index, polarization-dependent structural changes, and photoinduced dichroism [1, 2, 7, 8] are particularly noteworthy. The properties of chalcogenide glasses can be further influenced and tailored by changing composition, doping, and fabricating nano-composites [3, 4, 9–15]. Nanocomposite materials based on chalcogenide glasses may offer direct recording of surface reliefs with polarization dependent recording process [16].

Within the diverse family of chalcogenide glasses, Ga-Ge-Te alloys stand out due to their excellent far-infrared (FIR) properties [10, 17–20]. These include an exceptional optical transmission window ranging from 1.99 μm in the bandgap to 28 μm in the phonon region [10]. Additionally, in thin films, these alloys exhibit phase change-type optical memory, enabling rapid and reversible transitions between amorphous and crystalline states, with differing optical properties and conductivities [21, 22]. These attributes make them suitable for sensor applications as well [3, 4].

One should note that the possibility to control structural features of chalcogenide glasses and films is important to improve the characteristics of glasses and processes in them, including the photoinduced ones. Addition of Ga to GeTe alloys improves the amorphous phase stability (increases the crystallization temperature) and, hence, influences on the speed of crystallization and room temperature stability [9], and enhances the ability to form glass [3]. Therefore, better understanding of the structural properties of chalcogenide glasses is essential for optimizing their characteristics. In particular, the relief formation processes in composite nanomultilayer structures based on chalcogenide glasses are promising for direct information recording, data storage, and far-IR optics.

In the present report, amorphous Ga-Ge-Te alloys were studied by X-ray diffractometry and Raman spectroscopy.

2. Experimental details

The studied bulk Ga-Ge-Te alloys were prepared by the conventional melt quenching technique, the details of which can be found in [23]. In this work, we studied the following alloys: $Ge_{19}Te_{81}$ and $Ga_{7.9}Ge_{11.5}Te_{80.6}$ (Fig. 1).

The glassy domain in the Ga-Ge-Te system is limited to a small region centered on the $GeTe_4$-$GaTe_3$ pseudobinary line (Fig. 1) [10, 18]. It can be seen from Fig. 1 that the studied Ga-Ge-Te glass compositions lie within the glassy domain. The composition of the studied glasses was controlled using energy-dispersive X-ray spectroscopy (EDX). Fig. 2 shows an electronic microscope (EM) image of the surface of the studied $Ga_{7.9}Ge_{11.5}Te_{80.6}$ glass. The white rectangle in this figure indicates the probing area. Fig. 3 presents the EDX spectrum of the $Ga_{7.9}Ge_{11.5}Te_{80.6}$ glass.

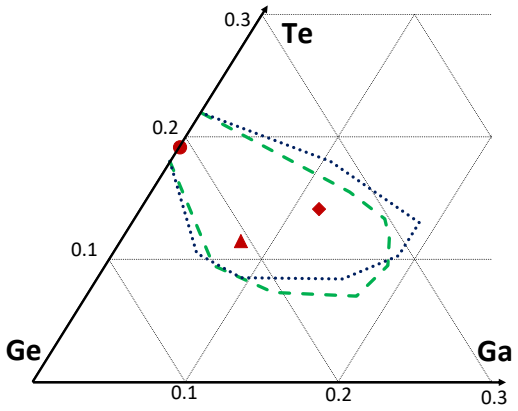

Fig. 1. Glassy domain limits in the Ga-Ge-Te system according to: - - - - [10] and ••••••• [18] and studied glass compositions: ● – $Ge_{19}Te_{81}$, ▲ – $Ga_{7.9}Ge_{11.5}Te_{80.6}$, and ◆ – $Ga_{11.7}Ge_{14.1}Te_{74.2}$ [23].

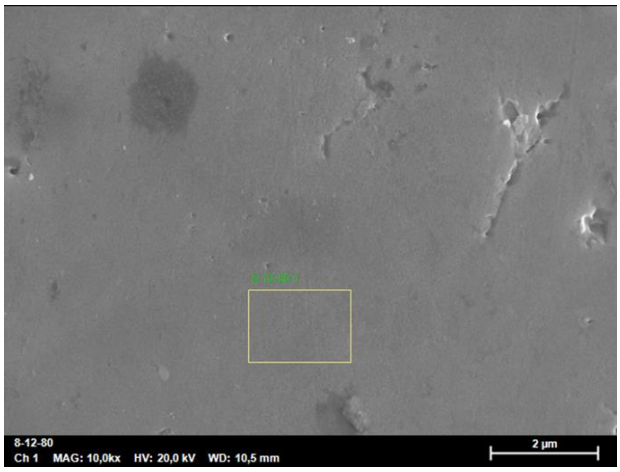

Fig. 2. EM image of the surface of the studied $Ga_{7.9}Ge_{11.5}Te_{80.6}$ glass. The rectangle indicates the probing area.

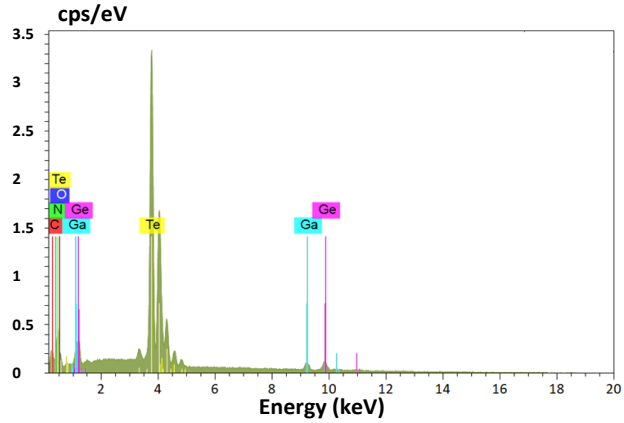

Fig. 3. EDX spectrum of the examined $Ga_{7.9}Ge_{11.5}Te_{80.6}$ glass. The abscissa axis represents the energy of X-ray quanta (keV), and the ordinate axis represents the fluorescence intensity (cps/ev).

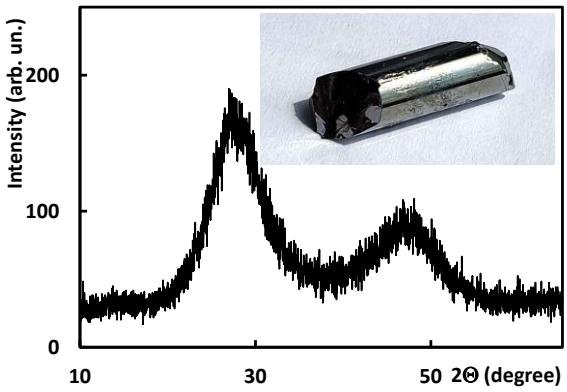

Fig. 4. XRD pattern of the $Ga_{7.9}Ge_{11.5}Te_{80.6}$ glass. Inset: bulk $Ga_{7.9}Ge_{11.6}Te_{80.6}$ glass.

X-ray diffraction (XRD) patterns of the samples were recorded with an X-ray diffractometer having the Bragg–Brentano geometry, using Cu Ka radiation source with $\lambda = 1.54178$ Å and mounted graphite monochromator for the diffracted beam. The diffraction data in the range of the scattering vector magnitudes Q between 0.4 and 8 Å, $Q = 4\pi\sin(\theta/\lambda)$, were collected. All the samples were examined in the transmission geometry. All the X-ray experiments were performed at ambient temperature. The XRD patterns of the studied Ga-Ge-Te alloys confirmed the amorphous nature of the samples. In Fig. 4, an XRD pattern of the $Ga_{7.9}Ge_{11.5}Te_{80.6}$ glass is shown as an example.

Radial distribution function (RDF(r)) is defined as the number of atoms lying at distances in the range $(r, r+dr)$ from the center of an arbitrary atom and is written as follows:

$$RDF(r) = 4\pi r^2 \rho(r). \quad (1)$$

Here, $\rho(r)$ is the density function, which represents an atomic pair correlation function. The average coordination number, N, in a spherical shell between

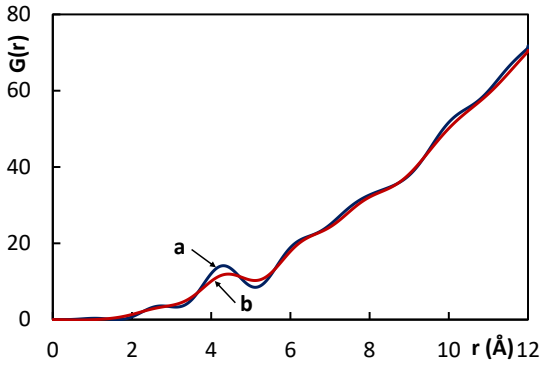

Fig. 5. Radial distribution functions of the studied Ga-Ge-Te glasses: a – $Ge_{19}Te_{81}$ and b – $Ga_{7.9}Ge_{11.5}Te_{80.6}$.

the radii r_1 and r_2 around any given atom can be calculated as the number of atoms in the area between r_0 and r, where r_0 is the first minimum of $4\pi r^2\rho(r)$. r_0 is the lower limit of r, below which $\rho(r)$ is equal to zero. The position of the first peak in radial distribution function gives the nearest-neighbour bond length r_1, and similarly, the position of the second peak gives the next neighbour distance r_2. The RDF yields only a limited amount of information, restricted essentially to the local structure around a given atom, *i.e.* the bond lengths and bond angles. Knowledge of both the bond lengths r_1 and r_2 yield the value of the bond angle θ given by [24]:

$$\theta = 2\sin^{-1}(r_2/2\cdot r_1). \qquad (2)$$

The experimental X-ray diffraction patterns were used for calculating the radial distribution functions (Fig. 5).

The short-range parameters are: number of the nearest neighboring atoms (coordination number), their type, the distance from them to the central atom (the radius r_1 of the first coordination sphere), and angular distribution of the atoms with respect to the central atom,

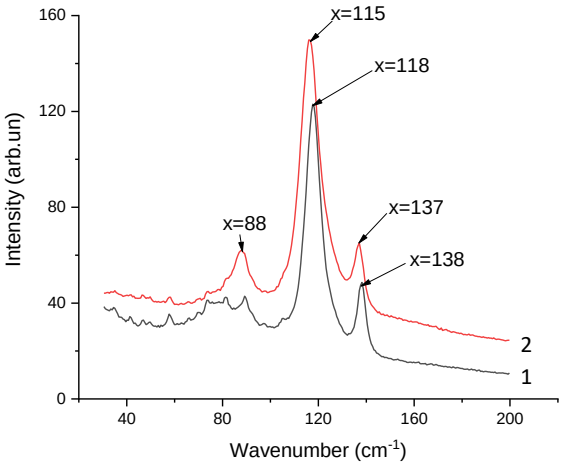

Fig. 6. Raman spectra of the Ga-Ge-Te glasses: *1* – $Ge_{19}Te_{81}$ and *2* – $Ga_{7.9}Ge_{11.5}Te_{80.6}$. For visual clarity, the second spectrum was shifted up by 10 arb. un. along the ordinate axis. The main bands are located near 88…90, 115…118, and 137…138 cm^{-1}.

which is determined by the chemical bond angles (valence angles φ). Such a definition limits short-range order to the first coordination sphere. At the same time, the short-range parameters define not only the first, but also, at least partially, the second coordination sphere. As can be seem from the expression (2), the radius of the second coordination sphere r_2 is defined by the radius of the first coordination sphere and the valence angle.

Raman and IR spectroscopy are widely used to study properties of functional materials [25–27]. Raman spectra of the studied Ga-Ge-Te glasses (Fig. 6) were measured at room temperature in the spectral range from 50 to 400 cm^{-1} by using a FRA-106 Raman attachment to Bruker IFS 88 applying a diode pump Nd:YAG laser of ca. 100 mW power and using a liquid nitrogen-cooled Ge detector with the resolution set to 1 cm^{-1} with 256 scans collected in each experiment. As reflected in Fig. 6, the main bands in the Raman spectra are located near 88…90, 115…118, and 137…138 cm^{-1}.

3. Results and discussion

The radial distribution functions (Fig. 5) obtained using the experimental X-ray diffraction patterns (Fig. 4) have provided the values of the nearest-neighbour bond length r_1 and second neighbour bond length r_2 (see Table 1).
Similar r_1 values were observed for the Ga-Ge-Te glasses of different compositions known from literature. The partial distribution functions (PDFs) for the Ga-Te, Ge-Te, and Te-Te in glassy $Ga_{11}Ge_{11}Te_{78}$ obtained in [28] had the following maxima (first PDF maxima): Ga-Te (2.63 Å), Ge-Te (2.65 Å), and Te-Te (2.83 Å). A strong second nearest-neighbour peak at 4.26 Å was the most pronounced feature of this Ga-Ge-Te composition. It was also noted that the well-defined PDF minima indicate that the mentioned bonds result from tetrahedral configurations around Ga and Ge, Ga-Ga, Ga-Ge, and Ge-Ge "wrong bonds" are not favored, and both Ga and Ge atoms have near four-fold coordination. For $Ga_{11.7}Ge_{14.1}Te_{74.2}$ glass, the r_2 value of 4.27 Å was obtained in [23]. For our studied compositions, we obtained 4.31 and 4.44 Å for r_2 (Table 1). In case of experimental determination of the structure of Ge-Ga-Te glasses, the main difficulty is that Ga and Ge have similar scattering properties both for neutrons and X-rays (Z_{Ge} = 32, Z_{Ga} = 31, b_{Ge}= 8.185 fm, b_{Ga} = 7.288 fm, where Z is the atomic number and b is the coherent neutron scattering length, respectively) [28]. The mean Ga-Te nearest-neighbour distance is between the Ge-Te and Te-Te bond lengths [29]. Therefore, another problem arises, namely sensitivity of the peak parameters

Table 1. Short-range parameters of the Ga-Ge-Te glasses.

Composition	r_1	r_2	r_2/r_1	θ
$Ge_{19}Te_{81}$	2.65	4.31	1.63	108
$Ga_{7.9}Ge_{11.5}Te_{80.6}$	2.65	4.44	1.68	114
$Ga_{11.7}Ge_{14.1}Te_{74.2}$ [23]	2.67	4.27	1.63	106

Table 2. Assignment of particular bands detected in the Raman spectra of Ga-Ge-Te, Ge-Te, Ga-Te, Te samples [23].

Wavenumber, cm^{-1}	Assignment	References
88	GeTe vibration modes	[37–41]
	Trigonal Te	[42]
92	Bending modes of $GeTe_4$ ($GaTe_4$) tetrahedral units	[38, 41]
104	Te modes	[42]
109	Symmetric Ga-Te breathing mode	[22]
115…125	Stretching mode of [$GeTe_4$], [$GaTe_4$] tetrahedral units	[33, 43]
120	Te-Te bonds	[44]
121	A1 mode of $GeTe_4$ tetrahedral unit	[45]
124…135	Corner-sharing (CS) or edge-sharing (ES) $GaTe_4$ tetrahedra breathing modes	[22]
141	Crystalline Te phase	[43, 46–48]
141	Te-Te bonds	[44]
150…155	Te-Te vibration bonds	[39, 46]
156	Te-Te stretching modes	[22]
160	Ge-Te vibration modes	[37–40]

to the ratio between the overlapping peaks. In order to obtain reliable information, it is necessary to study a concentration series because the uncertainty in the structural parameters for a single composition is relatively large. On the other hand, the main problem for a composition series is that the glassy domain in the Ga-Ge-Te system is limited to a small region (Fig. 2) and we have a small range of the concentration change. According to [28], the Ge-Te bond lengths for $Ge_{7.5}Ga_{7.5}Te_{85}$, $Ge_{12.5}Ga_{12.5}Te_{75}$ and $Ge_{14.3}Ga_{14.3}Te_{71.4}$ glasses are around 2.60 Å, while the Ga-Te bond length is 2.62…2.63 Å. The Ge-Te and Ga-Te bond lengths for $Ge_{10}Ga_{10}Te_{80}$ are 2.64 Å. The nearest-neighbour distances for the Ge-Ga-Te glasses $r_{Ge\text{-}Te}$ – 2.60…2.63 Å were estimated in [30]. The value of the Ge-Te bond length of 2.59 Å in the $Ge_{15}Ga_{10}Te_{75}$ glass is given in [29]. Experimental studies of the local order in binary Ge-Te glasses provide similar values of the Ge-Te bond lengths of 2.58…2.61 Å as obtained by combining diffraction and Extended X-ray Absorption Fine Structure (EXAFS) and Reverse Monte Carlo simulation (RMC) techniques [31]. The value $r_{Ge\text{-}Te}$ = 2.6 Å is obtained by using anomalous X-ray scattering and RMC [32].

The r_{GaTe} value (2.62…2.63 Å) found for the $Ge_xGa_xTe_{100-2x}$ glasses [28] is the same as that found experimentally for the Ge-Ga-Te glasses using EXAFS [30] and combination of experimental (diffraction, EXAFS) data with simulations (RMC and density functional theory) [33]. Somewhat longer Ga-Te bond length (2.67 Å) was found in [29] using first principles molecular dynamics simulations.

The Te-Te distances reported in the literature have a broad distribution. For amorphous Ge_xTe_{100-x}, the value of 2.76 Å was measured by neutron diffraction [34], and the values of 2.77…2.82 Å by EXAFS [35]. The Te-Te distances around 2.79…2.80 Å were reported for the Ge-Ga-Te glasses and Ge_xTe_{100-x} films [36].

The r_2/r_1 values of 1.63 and 1.68 (Table 1) are close to the typical respective value for a regular tetrahedron structure. The calculated values of the bond angle θ are also in good agreement with other published data on the Ga-Ge-Te alloys.

Raman spectra

The Raman spectra of the studied $Ge_{19}Te_{81}$ and $Ga_{7.9}Ge_{11.5}Te_{80.6}$ glasses (Fig. 6) have the main bands at 88, 118 and 138 cm^{-1}. Assignment of particular bands detected in the Raman spectra of the Ga-Ge-Te, Ge-Te, Ga-Te, and Te samples known from literature is presented in Table 2 [23].

The data presented in Table 2 show that for Te-Te, Ge-Te, and Ga-Te bonds, stretching vibrational frequencies are similar and, hence, the interpretation of the Raman spectra of Ga-Ge-Te glasses is not straightforward. The band at 88 cm^{-1} [37–41] in the spectrum is attributed in the literature to the oscillation modes of GeTe or trigonal Te. The main vibrational mode (symmetric breathing or stretching mode) of the $GaTe_{4/2}$ tetrahedra strongly overlaps with the corresponding band of the $GeTe_{4/2}$ tetrahedra due to the similar bond strengths of Ga-Te and Ge-Te bonds and similar atomic masses [33, 43]. The bending modes of $GaTe_{4/2}$ and $GeTe_{4/2}$ tetrahedra close to 92 cm^{-1} [38, 41], the tensile modes of tetrahedral units $GaTe_{4/2}$ and $GeTe_{4/2}$ in the region of 115 to 125 cm^{-1} [33, 43], and the oscillatory modes of tetrahedra $GaTe_{4/2}$ at 124…135 cm^{-1} are observed. The peak at 140 cm^{-1} corresponds to the oscillatory modes of Te-Te [22]. The observed bands in the Raman scattering spectra of the Ga-Ge-Te alloys show that such glasses contain different nanophases.

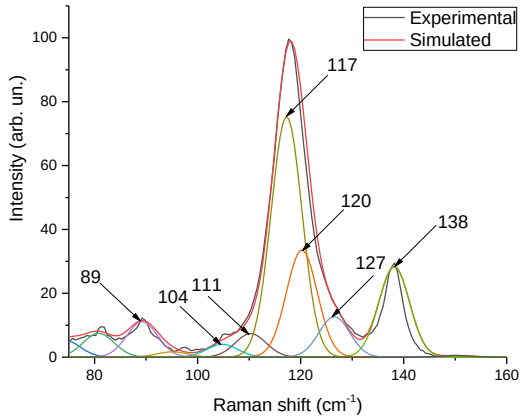

Fig. 7. Deconvolution of the Raman spectrum of the $Ge_{19}Te_{81}$ glass.

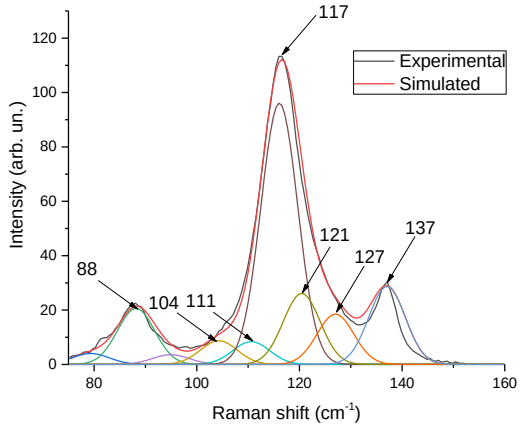

Fig. 8. Deconvolution of the Raman spectrum of the $Ga_{7.9}Ge_{11.5}Te_{80.6}$ glass.

The deconvolution of the Raman spectra of the studied Ga-Ge-Te glasses is shown in Figs 7 and 8. It can be seen from these figures that the spectra can be described in terms of vibrational modes of Ga-Te and Ge-Te glasses and films.

4. Conclusions

In this paper, amorphous $Ge_{19}Te_{81}$, and $Ga_{7.9}Ge_{11.5}Te_{80.6}$ alloys have been studied using X-ray diffraction and Raman spectroscopy. The experimental X-ray diffraction patterns confirmed amorphous nature of the obtained alloys. They were used for calculating radial distribution functions, which gave the positions of the nearest-neighbour peak r_1 = 2.65 Å and second nearest-neighbour peak r_2 = 4.31 and 4.44 Å. The obtained r_1 value has a good agreement with the known from the literature Ge-Te and Ga-Te bonds lengths. Similar r_1 values were also observed for the Ga-Ge-Te glasses of other compositions. The values of the ratio r_2/r_1 of 1.63 and 1.68 are close to the typical value for a regular tetrahedron structure. The observed bands in the Raman spectra of the studied Ga-Ge-Te samples show that such glass contains different nanophases. These bands may be explained in terms of the vibrational modes of Ga-Te and Ge-Te binary glasses and films.

References

1. Tanaka K. Light-induced anisotropy in amorphous chalcogenides. *Science*. 1997. **277**. P. 1786–1787. https://doi.org/10.1126/science.277.5333.1786.
2. Stronski A.V. Production of metallic patterns with the help of highresolution inorganic resists, in: *Microelectronic Interconnections and Assembly*, Springer Netherlands, Dordrecht, 1998. P. 263–293. https://doi.org/10.1007/978-94-011-5135-1_31.
3. Wilhelm A.A., Boussard-Plédel C., Coulombier Q. *et al*. Development of far-infrared-transmitting Te based glasses suitable for carbon dioxide detection and space optics. *Adv. Mater*. 2007. **19**. P. 3796–3800. https://doi.org/10.1002/adma.200700823.
4. Cui S., Boussard-Plédel C., Lucas J., Bureau B. Te-based glass fiber for far-infrared biochemical sensing up to 16 μm. *Opt. Express*. 2014. **22**. P. 21253. https://doi.org/10.1364/OE.22.021253.
5. Stronski A., Revutska L., Meshalkin A. *et al*. Structural properties of Ag–As–S chalcogenide glasses in phase separation region and their application in holographic grating recording. *Opt. Mater*. (*Amst*). 2019. **94**. P. 393–397. https://doi.org/10.1016/j.optmat.2019.06.016.
6. Gu H., Kang S., Fu Y. *et al*. High Seebeck coefficient inorganic $Ge_{15}Ga_{10}Te_{75}$ core/polymer cladding fibers for respiration and body temperature monitoring. *ACS Appl. Mater. Interfaces*. 2023. **15**. P. 59768–59775. https://doi.org/10.1021/acsami.3c13239.
7. Sanghera J.S., Aggarwal I.D. Active and passive chalcogenide glass optical fibers for IR applications: A review. *J. Non-Cryst. Solids*. 1999. **256-257**. P. 6–16. https://doi.org/10.1016/S0022-3093(99)00484-6.
8. Churbanov M.F., Scripachev I.V., Shiryaev V.S. *et al*. Chalcogenide glasses doped with Tb, Dy and Pr ions. *J. Non-Cryst. Solids*. 2003. **326–327**. P. 301–305. https://doi.org/10.1016/S0022-3093(03)00417-4.
9. van Pieterson L., Lankhorst M.H.R., van Schijndel M. *et al*. Phase-change recording materials with a growth-dominated crystallization mechanism: A materials overview. *J. Appl. Phys*. 2005. **97**. P. 083520. https://doi.org/10.1063/1.1868860.
10. Danto S., Houizot P., Boussard-Pledel C. *et al*. A family of far-infrared-transmitting glasses in the Ga–Ge–Te system for space applications. *Adv. Funct. Mater*. 2006. **16**. P. 1847–1852. https://doi.org/10.1002/adfm.200500645.
11. Stronski A., Kavetskyy T., Revutska L. *et al*. Stoichiometric deviations in bond distances in the mixed As_2S_3-As_2Se_3 system: Raman spectroscopy and EXAFS studies. *J. Non-Cryst. Solids*. 2019. **521**. P. 119533. https://doi.org/10.1016/j.jnoncrysol.2019.119533.
12. Baran J., Trzebiatowska M., Stronski A. *et al*. The influence of composition on short-range order of

amorphous As_2S_3-Sb_2S_3 chalcogenide alloys: A XRD and Raman study. *Funct. Mater*. 2020. **27**. P. 315–321. https://doi.org/10.15407/fm27.02.315.
13. Stronski A., Kavetskyy T., Revutska L. *et al*. Structural order in $(As_2S_3)_x(GeS_2)_{1-x}$ glasses. *J. Non-Cryst. Solids*. 2021. **572**. P. 121075. https://doi.org/10.1016/j.jnoncrysol.2021.121075.
14. Stronski A., Achimova E., Paiuk O. *et al*. Direct magnetic relief recording using $As_{40}S_{60}$: Mn–Se nanocomposite multilayer structures. *Nanoscale Res. Lett.* 2017. **12**. P. 286. https://doi.org/10.1186/s11671-017-2060-6.
15. Evdokimov I.I., Kurganova A.E., Velmuzhov A.P. Determination of the matrix composition of glasses of the Ga–Ge–Te–I system by inductively coupled plasma atomic emission spectrometry. *J. Analyt. Chem.* 2023. **78**. P. 644–651. https://doi.org/10.1134/S1061934823050040.
16. Stronski A., Achimova E., Paiuk O. *et al*. Optical and electron-beam recording of surface relief's using $Ge_5As_{37}S_{58}$–Se nanomultilayers as registering media. *J. Nano Res*. 2016. **39**. P. 96–104. https://doi.org/10.4028/www.scientific.net/JNanoR.39.96.
17. Zhang X.H., Calvez L., Seznec V. *et al*. Infrared transmitting glasses and glass-ceramics. *J. Non-Cryst. Solids.* 2006. **352**. P. 2411–2415. https://doi.org/10.1016/j.jnoncrysol.2006.03.029.
18. Bureau B., Danto S., Ma H.L. *et al*. Tellurium based glasses: A ruthless glass to crystal competition. *Solid State Sci*. 2008. **10**. P. 427–433. https://doi.org/10.1016/j.solidstatesciences.2007.12.017.
19. Xu H., He Y., Wang X. *et al*. Preparation of low-loss $Ge_{15}Ga_{10}Te_{75}$ chalcogenide glass for far-IR optics applications. *Infrared Phys. Technol.* 2014. **65**. P. 77–82. https://doi.org/10.1016/j.infrared.2014.03.008.
20. Cheng C., Wang X., Xu T. *et al*. Novel NaI improved Ge–Ga–Te far-infrared chalcogenide glasses. *Infrared Phys. Techn*. 2015. **72**. P. 148–152. https://doi.org/10.1016/j.infrared.2015.07.024.
21. Burr G.W., Breitwisch M.J., Franceschini M. *et al*. Phase change memory technology. *J. Vacuum Sci. Technol. B.* 2010. **28**. P. 223–262. https://doi.org/10.1116/1.3301579.
22. Bokova M., Tverjanovich A., Benmore C.J. *et al*. Unraveling the atomic structure of bulk binary Ga–Te glasses with surprising nanotectonic features for phase-change memory applications. *ACS Appl. Mater. Interfaces.* 2021. **13**. P. 37363–37379. https://doi.org/10.1021/acsami.1c09070.
23. Popovych M.V., Stronski A.V., Shportko K.V. Structural properties of $Ga_{18}Ge_{20.9}Te_{61.2}$ alloys. *Phys. Chem. Solid State*. 2022. **23**. P. 830–835. https://doi.org/10.15330/pcss.23.4.830-835.
24. Ramesh Rao N., Krishna P.S.R., Basu S. *et al*. Structural correlations in Ge_xSe_{1-x} glasses – a neutron diffraction study. *J. Non-Cryst. Solids*. 1998. **240**. P. 221–231. https://doi.org/10.1016/S0022-3093(98)00705-4.
25. Shportko K.V., Rueckamp R., Shoukavaya T.V. *et al*. Effect of the low temperatures on the Raman active vibrational modes in ZnP_2 and CdP_2. *Vib. Spectrosc.* 2016. **87**. P. 173–181. https://doi.org/10.1016/j.vibspec.2016.09.024.
26. Shportko K.V., Pasechnik Yu.A., Wuttig M. *et al*. Plasmon–phonon contribution in the permittivity of ZnP_2 single crystals in FIR at low temperatures. *Vib. Spectrosc.* 2009. **50**. P. 209–213. https://doi.org/10.1016/j.vibspec.2008.11.006.
27. Venger E.F., Pasechnik Yu.A., Shportko K.V. Reflection spectra of phosphides in the residual beams region. *J. Mol. Struct.* 2005. **744–747**. P. 947–950. https://doi.org/10.1016/j.molstruc.2004.11.046.
28. Pethes I., Piarristeguy A., Pradel A. *et al*. Short range order and topology of $Ge_xGa_xTe_{100-2x}$ glasses. *J. Alloys Compd*. 2020. **834**. P. 155097. https://doi.org/10.1016/j.jallcom.2020.155097.
29. Chaker Z., Ori G., Boero M. *et al*. First-principles study of the atomic structure of glassy $Ga_{10}Ge_{15}Te_{75}$. *J. Non-Cryst. Solids*. 2018. **498**. P. 338–344. https://doi.org/10.1016/j.jnoncrysol.2018.03.039.
30. Golovchak R., Calvez L., Bureau B., Jain H. Structural evolution of Ga-Ge-Te glasses by combined EXAFS and XPS analysis. *J. Chem. Phys.* 2013. **139**. P. 054508. https://doi.org/10.1063/1.4817332.
31. Jóvári P., Piarristeguy A., Pradel A. *et al*. Local order in binary Ge-Te glasses – An experimental study. *J. Alloys Compd*. 2019. **771**. P. 268–273. https://doi.org/10.1016/j.jallcom.2018.08.323.
32. Stellhorn J.R., Hosokawa S., Pilgrim W. *et al*. Short- and intermediate-range order in amorphous GeTe. *phys. status solidi* (*b*). 2016. **253**. P. 1038–1045. https://doi.org/10.1002/pssb.201552559.
33. Voleská I., Akola J., Jóvári P. *et al*. Structure, electronic, and vibrational properties of glassy $Ga_{11}Ge_{11}Te_{78}$: Experimentally constrained density functional study. *Phys. Rev. B*. 2012. **86**. P. 094108. https://doi.org/10.1103/PhysRevB.86.094108.
34. Kameda Y., Uemura O., Usuki T. Time-of-flight neutron diffraction study of amorphous and liquid Ge-Te alloys. *Mater. Trans. JIM.* 1996. **37**. P. 1655–1658. https://doi.org/10.2320/matertrans1989.37.1655.
35. Sen S., Joshi S., Aitken B.G., Khalid S. Atomic structure and chemical order in binary Ge–Te and As–Te glasses: A Te K-edge X-ray absorption fine structure spectroscopic study. *J. Non-Cryst. Solids*. 2008. **354**. P. 4620–4625. https://doi.org/10.1016/j.jnoncrysol.2008.05.048.
36. Piarristeguy A.A., Micoulaut M., Escalier R. *et al*. Structural singularities in Ge_xTe_{100-x} films. *J. Chem. Phys*. 2015. **143**. P. 074502. https://doi.org/10.1063/1.4928504.
37. Khoo C.Y., Liu H., Sasangka W.A. *et al*. Impact of deposition conditions on the crystallization kinetics of amorphous GeTe films. *J. Mater. Sci.* 2016. **51**. P. 1864–1872. https://doi.org/10.1007/s10853-015-9493-z.

38. Andrikopoulos K.S., Yannopoulos S.N., Voyiatzis G.A. *et al*. Raman scattering study of the a-GeTe structure and possible mechanism for the amorphous to crystal transition. *J. Phys.: Condens. Matter*. 2006. **18**. P. 965–979. https://doi.org/10.1088/0953-8984/18/3/014.
39. Andrikopoulos K.S., Yannopoulos S.N., Kolobov A.V. *et al*. Raman scattering study of GeTe and $Ge_2Sb_2Te_5$ phase-change materials. *J. Phys. Chem. Solids*. 2007. **68**. P. 1074–1078. https://doi.org/10.1016/j.jpcs.2007.02.027.
40. Mazzarello R., Caravati S., Angioletti-Uberti S. *et al*. Signature of tetrahedral Ge in the Raman spectrum of amorphous phase-change materials. *Phys. Rev. Lett*. 2010. **104**. P. 085503. https://doi.org/10.1103/PhysRevLett.104.085503.
41. Vigreux C., Vu Thi M., Escalier R. *et al*. Channel waveguides based on thermally co-evaporated Te–Ge–Se films for infrared integrated optics. *J. Non-Cryst. Solids*. 2013. **377**. P. 205–208. https://doi.org/10.1016/j.jnoncrysol.2012.11.037.
42. Manjón F.J., Gallego-Parra S., Rodríguez-Hernández P. *et al*. Anomalous Raman modes in tellurides. *J. Mater. Chem. C*. 2021. **9**. P. 6277–6289. https://doi.org/10.1039/D1TC00980J.
43. Dong N., Chen Y., Wei N. *et al*. Optical and structural properties of Ge-Ga-Te amorphous thin films fabricated by magnetron sputtering. *Infrared Phys. Techn*. 2017. **86**. P. 181–186. https://doi.org/10.1016/j.infrared.2017.09.008.
44. Pine A.S., Dresselhaus G. Raman Spectra and lattice dynamics of tellurium. *Phys. Rev. B.* 1971. **4**. P. 356–371. https://doi.org/10.1103/PhysRevB.4.356.
45. Torrie B.H. Raman spectrum of tellurium. *Solid State Commun*. 1970. **8**. P. 1899–1901. https://doi.org/10.1016/0038-1098(70)90343-1.
46. Sen S., Gjersing E.L., Aitken B.G. Physical properties of $Ge_xAs_{2x}Te_{100-3x}$ glasses and Raman spectroscopic analysis of their short-range structure. *J. Non-Cryst. Solids*. 2010. **356**. P. 2083–2088. https://doi.org/10.1016/j.jnoncrysol.2010.08.013.
47. Němec P., Nazabal V., Dussauze M. *et al*. Ga–Ge–Te amorphous thin films fabricated by pulsed laser deposition. *Thin Solid Films*. 2013. **531**. P. 454–459. https://doi.org/10.1016/j.tsf.2013.01.096.
48. Sun J., Nie Q., Wang X. *et al*. Structural investigation of Te-based chalcogenide glasses using Raman spectroscopy. *Infrared Phys. Techn*. 2012. **55**. P. 316–319. https://doi.org/10.1016/j.infrared.2012.03.003.

Authors' contributions

Stronski A.V.: conceptualization, analysis, writing – review & editing.
Shportko K.V.: conceptualization, analysis, writing – review & editing.
Kochubei H.K.: investigation, formal analysis.
Popovych M.V.: investigation, formal analysis.
Lotnyk A.A.: investigation, formal analysis.

Authors and CV

Alexander Stronski, Doctor of Sciences in Physics and Mathematics, Leading Researcher at the Department of Optoelectronics, V. Lashkaryov Institute of Semiconductor Physics, NAS of Ukraine. He is the author of three monographs, one chapter in a book and over 400 scientific works. His main research activity is in the field of materials science, optoelectronics, optical elements, and optical properties and photostimulated processes in disordered materials and composite nanostructures based on them.
E-mail: alexander.stronski@gmail.com
https://orcid.org/0000-0002-5096-3740

Kostiantyn Shportko defended his PhD thesis in Physics and Mathematics (Physics of Semiconductors and Dielectrics) in 2004 and Doctor of Sciences (Solid State Physics) thesis in 2020. He is a Senior Researcher at the Department of Sensor Systems at the V. Lashkayov Institute of Semiconductor Physics, NAS of Ukraine. He is the author of over 100 scientific works. His main research activity is in the field of materials science and optical properties of functional materials.
E-mail: k.shportko@ukr.net,
https://orcid.org/0000-0001-6813-4871

Mykhailo Popovych obtained his MS degree in Applied Physics and Nanomaterials at the National Technical University of Ukraine "Igor Sikorsky Kyiv Polytechnic Institute" in 2018. He is a Junior Researcher at the Department of Optoelectronics at the V. Lashkayov Institute of Semiconductor Physics, NAS of Ukraine. He is the co-author of 18 scientific works. His main research activity is in the field of disordered materials and composite nanostructures based on them. E-mail: Niva94@ukr.net

Hanna Kochubei obtained her MS degree in Applied Physics and Nanomaterials at the National Technical University of Ukraine "Igor Sikorsky Kyiv Polytechnic Institute" in 2022. She is a PhD student at the V. Lashkayov Institute of Semiconductor Physics, NAS of Ukraine. She is the co-author of 3 scientific works.
Her main research activity is in the field of disordered materials, their structural and other properties, and composite nanostructures based on them.
E-mail: kochubei.hanna@gmail.com

Andriy Lotnyk earned his Diploma in Physics from the V. Karazin Kharkiv National University, Ukraine, in 2002. He completed his PhD work at the Max Planck Institute of Microstructure Physics, Germany, and defended the PhD thesis at the Martin Luther University Halle-Wittenberg in 2007. In 2022, he defended his habilitation thesis at the Leipzig University, Germany, earning the Dr. habil. degree. Since 2011, he has led the Leipziger nanoAnalytics center at the IOM Leipzig. He is the author and co-author of over 150 peer-reviewed publications. His current research focuses on growth and properties of thin films, structure analysis using electrons and X-rays, and laser-beam-induced modification of thin films.
E-mail: andriy.lotnyk@iom-leipzig.de, https://orcid.org/0000-0002-0000-9334

Дослідження склоподібних сплавів Ga-Ge-Te за допомогою рентгенівської дифракції та спектроскопії комбінаційного розсіювання світла

А.В. Стронський, К.В. Шпортько, Г.К. Кочубей, М.В. Попович, A.A. Lotnyk

Анотація. Структуру та вібраційні властивості склоподібних сплавів $Ge_{19}Te_{81}$ та $Ga_{7.9}Ge_{11.5}Te_{80.6}$ вивчено за допомогою рентгенівської дифракції та спектроскопії комбінаційного розсіювання світла. Аморфний характер отриманих сплавів підтверджено експериментальними рентгенівськими дифракційними картинами, які були використані для розрахунків радіальних функцій розподілу, що дали положення найближчого сусіднього піка r_1 – 2,65 Å і другого найближчого сусіднього піка r_2 – 4,31 і 4,44 Å. Отримані значення r_1 добре узгоджуються з відомими з літератури для довжин зв'язків Ge-Te і Ga-Te, аналогічні значення r_1 спостерігалися для стекол Ga-Ge-Te інших складів. Значення співвідношення r_2/r_1 1,63 і 1,68 близькі до типового значення для правильної структури тетраедра. Спостережувані смуги в спектрах комбінаційного розсіювання світла вивчених зразків Ga-Ge-Te показують, що такі скла містять різні нанофази і можуть бути пояснені в термінах коливальних мод бінарних стекол та плівок Ga-Te і Ge-Te.

Ключові слова: рентгенівська дифракція, спектроскопія комбінаційного розсіювання світла, склоподібні сплави Ga-Ge-Te.